

Phase diagrams of cuprates and pnictides as a key to the HTSC mechanism

K. V. Mitsen and O. M. Ivanenko

Lebedev Physical Institute, 119991 Moscow, Russia

We propose a model of heterovalent doping that enables determination of the superconductivity dome position on phase diagram of a particular HTSC compound proceeding from its crystal structure and dopant location. As it follows from the model, the observed similarity of the phase diagrams of cuprates and pnictides is due to the mechanism of superconductivity common for both HTSC families, the basis of which is the pairing of carriers on certain two-centre atomic complexes - Heitler-London (HL) centres. Each HL centre is formed in the basal plane between two dopant projections being at a certain distance one from the other. For a superconducting domain to be formed, HL centres should make up a percolation cluster. We calculated the concentration ranges corresponding to the formation of a percolation cluster of HL centres for a number of well investigated cuprates and pnictides and found an excellent coincidence of these ranges with the positions of the superconductivity domes on the corresponding phase diagrams. We consider this coincidence to be a confirmation of the model, which assumes the realization of the mechanism of superconducting pairing at HL centres.

PACS numbers: 74.25.Dw, 74.62.Dh, 74.70.Xa, 74.72.-h

I. INTRODUCTION

The nature of the normal state and the mechanism of superconductivity in two high-temperature superconductor families – cuprates and pnictides – has remained an issue of animated discussion. Undoped cuprates, as it follows from the experiment and as supported by band calculations, possess electronic structures essentially other than pnictides. Still, the differences in their electronic structures notwithstanding, these compounds exhibit a number of similar properties; in particular, they demonstrate an evident similarity of their phase diagrams. This gives an impression of a common and rather rough mechanism that acts irrespectively of fine band-structure details and provides for superconducting pairing in these materials.

Guided by this idea, we outline some common features of these compounds, which, in our mind, are important for the existence of this common mechanism:

(1) *Low concentration of charge carriers.* Even at an optimal doping, the carrier concentration in cuprates and pnictides is lower than 10^{22} cm^{-3} , which corresponds to an average distance of $r_s > 0.4 \text{ nm}$ between the carriers and exceeds the distance between the anion and the cation. This means that the interaction inside the cell is essentially unshielded, which enables the existence of well-defined charge transfer (CT) excitons [1].

(2) *High ionicity of cuprates and pnictides,* which suggests a large contribution of Madelung volume energy E_M to the electronic structure of basal planes and the possibility to locally change the electronic structure by doping with localized carriers.

(3) *Existence of a band gap $\Delta_b \sim 2 \text{ eV}$ in undoped cuprates and pnictides* that separates the occupied anion band from unoccupied states of the cation band. That is, an approximately the same energy of $\sim 2 \text{ eV}$ is required to transfer an electron from an anion to a cation both in cuprates and pnictides.

We believe that exactly these features determine the anomalous properties of cuprates and pnictides; we propose a model that describes changes in their electronic structure under doping and enables predicting the range of superconductivity dome on the phase diagram of any particular HTSC compound proceeding from its crystal structure and type of doping. Based on the proposed model, we will determine the superconductivity dome positions for the well investigated cuprates and pnictides and will compare them with the experimental phase diagrams. We will also discuss the nature of current carriers in these compounds in normal state and will propose an electron pairing mechanism, which we consider to be responsible for superconductivity in both HTSC families.

II. MODEL OF DOPING

Figures 1a,b show an arrangement of anions and cations (their projections, to be more exact) in the basal planes of cuprates and pnictides. In cuprates, Cu and O ions are in the same plane; in pnictides, Fe ions are in the plane and As ions are at the vertices of the regular tetrahedra such that their projections form a square sublattice in the basal plane.

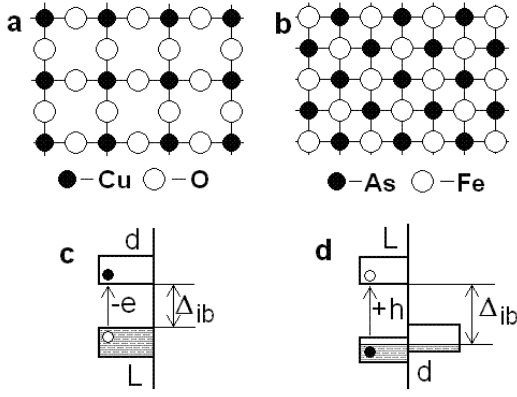


Figure 1. (a,b) Arrangement of the projections of anions and cations in the basal planes of cuprates (a) and pnictides (b); (c) the band structure of undoped cuprates in electron representation; (d) the band structure of undoped pnictides in hole representation. Bands d and L are cation and anion bands, respectively. The gap Δ_{ib} is ~ 2 eV both for cuprates and pnictides.

Figures 1 c,d schematically show the band structures of undoped cuprates (in electron representation) (c) and undoped pnictides (in hole representation) (d). Here, d is the conduction band formed by the orbitals of d cations; L is the valence band formed by the orbitals of anions (ligands). It is noteworthy that an approximately the same energy $\Delta_{ib} \sim 2$ eV should be expended for the transfer of an electron to conduction band d (in cuprates) and of a hole to band L (in pnictides).

At the same time exciton-like excitation is also possible, which has a lower energy $\Delta_{ct} < \Delta_{ib}$ and corresponds to the local transfer of an electron (hole) from an anion (cation) to the nearest cation (anion) (Fig. 2a,b) to form the bound state (of a CT exciton).

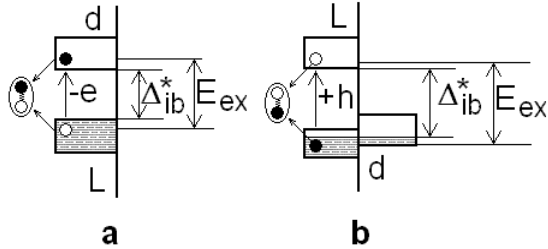


Figure 2. Formation of a CT exciton in cuprates (a) and pnictides (b). To form the CT exciton, the band gap Δ_{ib} should be reduced to $\Delta_{ib} = \Delta_{ib}^* < E_{ex}$, CT exciton binding energy.

If Δ_{ib} is somehow gradually decreased, we shall first arrive to a state with $\Delta_{ib} = \Delta_{ib}^*$, in which $\Delta_{ct} = 0$ (i.e., $\Delta_{ib}^* \leq E_{ex}$, where E_{ex} is CT exciton binding energy). If Δ_{ib} is decreased homogeneously, the condition $\Delta_{ct} = 0$ will be satisfied for the entire basal plane. If we locally suppress Δ_{ib} in some regions, a continuous cluster of the phase with $\Delta_{ct} = 0$ will emerge at an excess of the percolation threshold over those regions.

With d- and L-orbitals hybridized, the band states interact resonantly with the CT exciton states, i.e., two-particle transitions to and fro become possible between two one-particle states (L electron + d hole) and an exciton two-particle state (d electron + L hole). Therefore, electron states on the level of chemical potential (in cuprates) and hole states (in pnictides) should be considered as a superposition of purely band and exciton states. Herewith, the events corresponding to the generation of a CT exciton are, in cuprates, an electron on the central Cu cation in CuO_4 plaquette, and a hole distributed over four surrounding anions of O; and, in pnictides, a hole on the As anion in AsFe_4 plaquette and an electron distributed over four surrounding cations of Fe. This hydrogen-like ionic complex (CuO_4^- or AsFe_4^- plaquette), in which a CT exciton, resonantly interacting with the band states, can be formed, will be called an EXION.

Our next statement is that, the HTSC phase is exion phase (with $\Delta_{ct} = 0$), where pairs of exions centred on the nearest cations of Cu (in cuprates) or anions of As (in pnictides) form so called HL centres, which determine the normal and superconducting properties of these compounds.

Leaving the possible mechanisms of conductivity (and superconductivity) in a system with $\Delta_{ct} = 0$ for further discussion, we would now like to show that, for various HTSC compounds, regions of the existence of percolation cluster of HL centres as a function of doping coincide with high-temperature superconductivity regions on their phase diagrams. For this purpose, we will first consider how the doping transforms the band structure of cuprates and pnictides (Fig. 2), leading to the formation of exions and HL centres.

As the gap Δ_{ib} in cuprates and pnictides is largely determined by Madelung energy E_M , we need to locally decrease the value of E_M to form an exion centred on a given (Cu or As) ion. Hypothetically, this can be done by arranging additional localized charges of respective value and sign either on the central (Cu or As) ion or on one of four surrounding ions (of O or Fe), or else in the immediate vicinity from them. Interestingly, exactly this mechanism of decreasing Δ_{ib} appears to be realized in HTSCs under doping.

We shall proceed from the premise that introduction of a dopant ion into the crystal lattice is accompanied with the emergence, in the basal plane or outside it, of an additional carrier (an electron or a hole). In the process of delocalization the doped carrier, in accordance with the neighbourhood symmetry, "passes" the fractional charge $q^* \approx \pm|e|/4$ to corresponding orbitals of the nearest ions.

In turn, charge q^* emerging on each of four Cu (As) ions (Fig. 3a) locally decreases Madelung energy. Herewith, we neglect the effect of the charge of the dopant, which is at a larger distance. In turn, a local decrease of Madelung energy reduces the gap Δ_{ib} for the transition of an electron (a hole) to each of four ions of Cu (As) from the surrounding ions of O (Fe). As estimates show [2], at

$q^* \approx |e|/4$ and the existing interatomic distances this decrease is ~ 1 eV and, in our assumption, is sufficient to fulfill the condition $\Delta_{ct} = 0$, i.e., to form an exion on these ionic complexes.

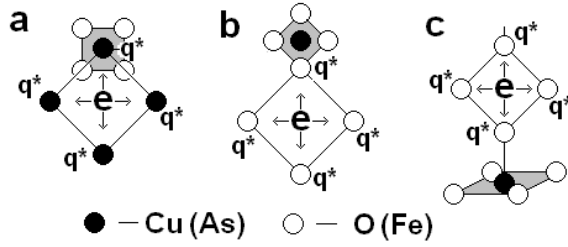


Figure 3. Formation of exions and self-localization of doped charges in cuprates and pnictides. Exions, forming on CuO_4 or AsFe_4 plaquettes, are shaded. (a) hole doping in pnictides or electron doping in cuprates; (b) hole doping in cuprates or electron doping in pnictides; (c) a dopant and a doped charge outside the basal plane (YBCO, BSCO etc.)

As each exion is bound by Coulomb attraction to doped charge q^* , the doped carrier self-localizes in the muffin-tin sphere of the substituted site. The conclusion of the localization of doped carriers in the nearest vicinity of the dopant ion (both in cuprates and pnictides) is supported by the results of Refs. [3-7].

Thus, the localization boundary of the doped carrier is determined by the condition that the same charge q^* ($\sim \pm |e|/4$) sufficient for exion formation be at this boundary per each anion (cation). In fact, we produce a trion complex where the doped carrier is bound to four CT excitons that interact resonantly with the band states. This exion formation mechanism (Fig. 3a) is realized in electron-doped cuprates and hole-doped pnictides.

In the case shown in Fig. 3b, doped charge q^* occurring at each of four O (Fe) ions locally decreases Madelung energy and forms an exion in the next ion square centred on the nearest Cu (As) ion, because only these ions can be exion centres. This scheme is realized for hole-doped cuprates and electron-doped pnictides.

Figures 3a,b consider the cases when a doped carrier is in the basal plane. However, it is possible that doped charge q^* localizes outside the plane (Fig. 3c), e.g., on apical ions of oxygen, as it takes place in YBCO and other two-plane cuprates. This charge also decreases electron energy on the nearest Cu ion by the required value and thereby forms an exion in the plane of CuO_2 .

Thus, according to the above said, exions that are simultaneously traps for charges q^* are formed around the dopant projection on the basal plane. Herewith, a pair of exions centred on the nearest cations (in cuprates) or anions (in pnictides) forms an HL centre on which, as we assume, two electrons (two holes) can form a bound state. Let us now consider the conditions of HL centre formation as exemplified by well investigated HTSCs and, proceeding from this, let us try to determine the superconductivity dome positions on their phase diagrams.

As each HL centre consists of two exions centred on two adjacent cations (in cuprates) or anions (in pnictides), the percolation cluster of HL centres may exist only at a certain distance between the dopant projections. This determines the range of dopant concentrations within which the maximum number of HL centres can be formed. Herewith, the concentration range conforming to the superconductivity dome for compounds of a given crystal structure and a given type of doping will correspond to the dopant concentration range within which the formation of a percolation network of HL centres is possible.

Guided by the above considerations, let us now pass on to determination of superconductivity domes for particular HTSCs, whose experimental phase diagrams are specified (Fig. 4).

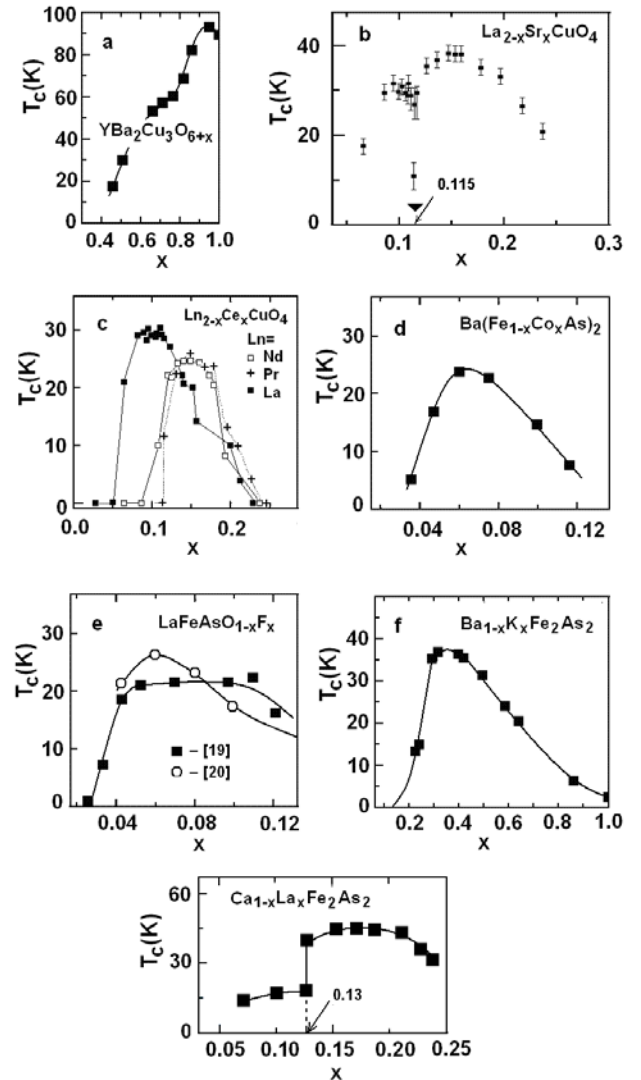


Figure 4. Experimental superconducting phase diagrams for some of well specified cuprates and pnictides. a) $\text{YBa}_2\text{Cu}_3\text{O}_{6+x}$ [8]; b) $\text{La}_{2-x}\text{Sr}_x\text{CuO}_4$ [9]; c) $\text{Ln}_{2-x}\text{Ce}_x\text{CuO}_4$ [10]; d) $\text{Ba}(\text{Fe}_{1-x}\text{Co}_x\text{As})_2$ [11]; e) $\text{LaFeAsO}_{1-x}\text{F}_x$ [12,13]; f) $\text{Ba}_{1-x}\text{K}_x\text{Fe}_2\text{As}_2$ [14]; g) $\text{Ca}_{1-x}\text{La}_x\text{Fe}_2\text{As}_2$ [15].

III. DETERMINATION OF SUPERCONDUCTIVITY DOMES

A. $\text{La}_{2-x}\text{Sr}_x\text{CuO}_4$

In the cases when a doped charge is in the basal plane, for an HL centre between two dopant projections to emerge it is necessary that they be at some fixed distances l_{HL} apart. The maximal number of HL centres in the basal plane can be formed if dopant projections are ordered into a square superlattice with parameter l_{HL} . The concentration of dopants, $x_{\text{max}}=1/l_{\text{HL}}^2$, corresponding to the formation of a square superlattice with parameter l_{HL} , will be taken for the upper boundary of the optimal doping region. This boundary corresponding to the maximal concentration of HL centres also corresponds to the maximum T_c . For the lower boundary, $x_{\text{min}}=0.593/l_{\text{HL}}^2 \approx 0.6/l_{\text{HL}}^2$, we will conventionally take a dopant concentration corresponding to the site percolation threshold on a square superlattice with parameter l_{HL} [16]. This choice is determined by the fact that the existence of physically significant domains with the percolation network of dopant projections, spaced by a distance of l_{HL} one from another, is possible only at

$$0.6/l_{\text{HL}}^2 < x < 1/l_{\text{HL}}^2.$$

This does not mean that the percolation cluster on a superlattice with parameter l_{HL} should occupy the entire crystal, but that such domains can exist within only this concentration range. Herewith, a superconductivity in the entire crystal emerges owing to the Josephson coupling between such domains.

The specific shape of $T_c(x)$ curve in a superconductivity dome is defined by the realizability of different types of dopant ordering in a given crystal structure [17-19].

In the case of $\text{La}_{2-x}\text{Sr}_x\text{CuO}_4$, the doped hole emerging at the substitution of Sr^{2+} for La^{3+} is in the CuO_2 plane (Fig. 5) and its charge is distributed over four oxygen ions pertaining to the oxygen octahedron adjacent to Sr ion [3,4]. Each of the four fractional charges q^* on oxygen ions forms an exion in the next ion square centred on the nearest Cu cation (Fig. 3b). It is readily seen that only two variants of the relative arrangement of two nearest projections of Sr on the CuO_2 plane are possible so that they could form an HL centre (Figs. 5a and 5b). These cases correspond to two possible distances between them, $l = 3a$ and $l = a\sqrt{5}$ (a , the lattice parameter). The HL centres formed in the CuO_2 plane and representing exion pairs centred on Cu ions (double circles) are encircled with solid lines. Note that in an intermediate case when the distance between the Sr projections is $l = a\sqrt{8}$ (Fig. 5c), no exion pair is formed on neighbouring Cu ions.

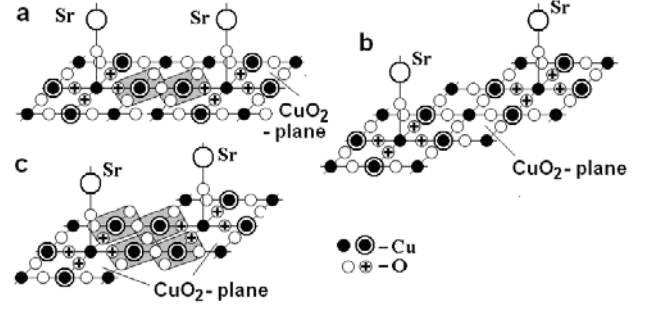


Figure 5. Formation of exions and HL centres in $\text{La}_{2-x}\text{Sr}_x\text{CuO}_4$ at various distances between dopant projections: (a) $l = 3a$; (b) $l = a\sqrt{5}$; (c) $l = a\sqrt{8}$. Double circles are Cu ions, which are exion centres. Exions that form HL centres are shaded.

In accordance with two different variants of HL centre formation, the phase diagram of $\text{La}_{2-x}\text{Sr}_x\text{CuO}_4$ is expected to have two regions of optimal doping at $0.066 < x < 0.11$ and at $0.12 < x < 0.2$ (corresponding to the ordered arrangement of Sr projections onto 3×3 and $\sqrt{5} \times \sqrt{5}$ superlattices). Note that the experimental value of the upper optimal concentration, $x = 0.15$ (optimal in the sense of the magnitude of T_c) differs from the expected value, $x = 1/5$, though a jumplike decrease of the volume of the superconducting phase is observed namely at $x = 1/5$ [20]. We explain this discrepancy by the formation of clusters of normal metal at $x > 0.15$ [21]. Within the interval of $0.11 < x < 0.12$, domains with the percolation network of HL centres cannot exist. This is the so-called 1/8 anomaly, which, however, takes place not at $x = 0.125$ but at $x = 0.115$, in agreement with experimental data (Fig.4b) [9,22]. Within the interval of $0.11 < x < 0.12$, due to the absence of HL centre percolation, material includes non-conducting regions, which makes it possible to observe in this concentration range (and in it only) a static magnetic texture imitating stripes [23].

C. $\text{Ln}_{2-x}\text{Ce}_x\text{CuO}_4$

In the electron-doped HTSC $\text{Ln}_{2-x}\text{Ce}_x\text{CuO}_4$ the doped electron emerging at the substitution of Ce^{4+} for Ln^{3+} is in the CuO_2 plane (Fig. 6) and its charge is distributed over four Cu ions. In accordance with Fig. 3a, four external ions of Cu are exion centres. Similar to $\text{La}_{2-x}\text{Sr}_x\text{CuO}_4$, two types of HL centres and, respectively, two regions of optimal doping – $0.066 < x < 0.11$ and $0.12 < x < 0.2$ – within which a percolation network of HL centres can be formed, are possible in this compound (Fig.6 a,b). However, on the phase diagrams of $\text{Nd}_{2-x}\text{Ce}_x\text{CuO}_4$ and $\text{Pr}_{2-x}\text{Ce}_x\text{CuO}_4$ (Fig. 4c [24]) only one superconducting dome is observed with a T_c maximal at $x = 0.15$ and falling to zero at an increase of $x > 0.2$.

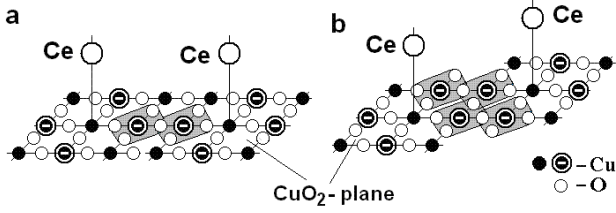


Figure 6. Formation of exions and HL centres in $\text{Ln}_{2-x}\text{Ce}_x\text{CuO}_4$ at various distances between dopant projections: (a) $l = 3a$; (b) $l = a\sqrt{5}$; double circles are Cu ions, which are exion centres. Exions that form HL centres are shaded.

We associate this discrepancy with a low degree of order of Ce ions in the superlattice owing to the proximity of the atomic radii of Nd, Pr and Ce ($r_{\text{Nd}} \approx r_{\text{Pr}} \approx r_{\text{Ce}} \approx 0.185$ nm [25]). At the same time, on the phase diagram of $\text{La}_{2-x}\text{Ce}_x\text{CuO}_4$ ($r_{\text{La}} \approx 0.195$ nm [25]) one can clearly see two superconducting domes in the expected intervals with the local T_c maxima at $x = 0.11$ and $x = 0.15$ (Fig. 4c [10]), as in $\text{La}_{2-x}\text{Sr}_x\text{CuO}_4$.

C. $\text{YBa}_2\text{Cu}_3\text{O}_{6+x}$

The parent compound $\text{YBa}_2\text{Cu}_3\text{O}_6$ is doped by introducing excess oxygen into the plane of the chains. In the case when three positions in the chain in succession are occupied by oxygen ions (Fig. 7), each of the formed oxygen squares holds one hole (the circled plus symbol), each of which is distributed over four oxygen ions of this square. Herewith, additional positive charges $\approx q^*$ ($\approx +|e|/4$) emerge on oxygen ions nearest to the in-plane Cu ions (double circles). The HL centres formed in both CuO_2 planes and representing pairs of exions centred on Cu ions (double circles) are encircled with solid lines. When positions in chains are completely occupied by oxygen, each pair of adjacent cations surrounded by anions will be an HL centre.

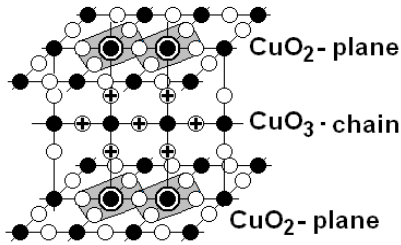


Figure 7. Formation of exions and HL centres in $\text{YBa}_2\text{Cu}_3\text{O}_{6+x}$. With three oxygen positions in the chain in succession occupied by oxygen ions, each of the two formed oxygen squares has one hole, each of which is distributed over four oxygen ions of this square. Herewith, additional positive charges $\approx q^*$ ($\approx +|e|/4$) emerge on the apical oxygen ions nearest to the in-plane Cu ions (double circles). This is sufficient to form on these cations two exions in each CuO_2 plane that make up two HL centres (shaded).

To form a single HL centre in the CuO_2 plane it is necessary to fill three successive positions in the chain with excess oxygen. Herewith, a continuous cluster of HL centres is formed at an excess of the percolation threshold by the linear triples of oxygen ions in the plane of the chains. As the calculation shows [26], the percolation threshold in this case corresponds to the excess oxygen concentration of $x \geq 0.8$. Thus, the region of optimal doping for $\text{YBa}_2\text{Cu}_3\text{O}_{6+x}$ is within the interval of $0.8 < x < 1$, in accordance with the experiment (Fig. 4a [8]). We should note that $\text{YBa}_2\text{Cu}_3\text{O}_7$ is the only case when doping can realize condition $\Delta_{\text{ct}} = 0$ for the entire basal plane. In the case of, e.g., another double-plane cuprate $\text{Bi}_2\text{Sr}_2\text{CaCu}_2\text{O}_{8+x}$, where $0 < x < 2$, inhomogeneous filling of excess oxygen positions leads to various charges q^* on the apical ions of oxygen, a consequence of which is the co-existence of underdoped and overdoped regions in one basal plane, together with optimally doped regions.

D. $\text{Ba}(\text{Fe}_{1-x}\text{Co}_x\text{As})_2$

In this compound, doping is performed by substituting Co atoms for Fe in the basal plane (Fig. 8). An additional electron emerging at the substitution imparts charge q^* ($\approx -|e|/4$) to each of four surrounding Fe ions (Fig. 8a). Basically, two kinds of HL centres (Figs. 8b and 8c) with the same distance between As anions are possible. Still, we think that the HL centre in Fig. 8b is more efficient, as in this case electrons will remain longer between As anions.

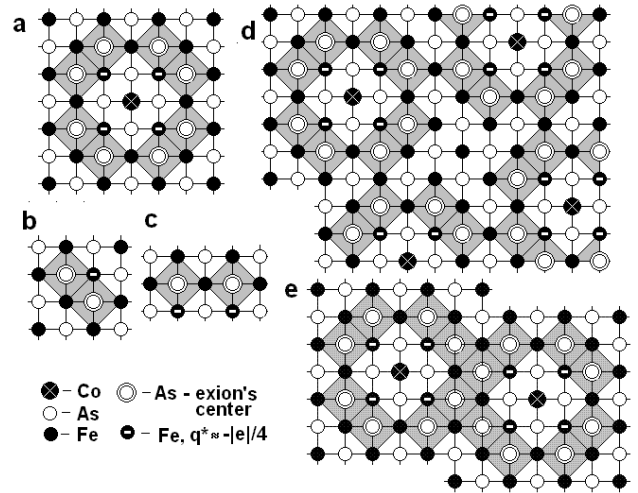


Figure 8. Formation of exions and HL centres in $\text{Ba}(\text{Fe}_{1-x}\text{Co}_x\text{As})_2$. Open circles indicate projections of As ions at the vertices of the tetrahedra onto the Fe plane; a, formation of exions around the Co ion; b, c, possible types of HL centres in $\text{Ba}(\text{Fe}_{1-x}\text{Co}_x\text{As})_2$; d, e, formation of percolation clusters of HL centres on $\sqrt{2} \times \sqrt{2}$ and $\sqrt{13} \times \sqrt{13}$ square superlattices. Exions that form HL centres are shaded.

At an ordered arrangement of dopants in a $\sqrt{20} \times \sqrt{20}$ superlattice we will have a percolation network of HL centres (Fig. 8b). A corresponding concentration of optimal doping is $x = 0.05$, and the concentration corresponding to the percolation threshold is $x = 0.03$, which is in good agreement with the experimental phase diagram of $\text{Ba}(\text{Fe}_{1-x}\text{Co}_x\text{As})_2$ (Fig. 4f). It is readily seen that other distances between dopants, ensuring the formation of HL centres between them, are possible within the interval of $a\sqrt{13} \leq l \leq a\sqrt{20}$, too (Fig. 8e). This interval corresponds to the concentration range of $0.03 \leq x \leq 0.08$ in agreement with experimental data (Fig. 4d [11]).

E. $\text{LaFeAsO}_{1-x}\text{F}_x$

In this compound, at the substitution of fluorine for oxygen one electron is doped into the basal plane. The projection of F ion onto the basal plane coincides with the position of Co ion in Fig. 8a. As a consequence, the symmetry of doped charge distribution in $\text{LaFeAsO}_{1-x}\text{F}_x$ will be similar to that in $\text{Ba}(\text{Fe}_{1-x}\text{Co}_x\text{As})_2$ (Fig. 8a). Therefore, the phase diagrams of $\text{LaFeAsO}_{1-x}\text{F}_x$ and $\text{Ba}(\text{Fe}_{1-x}\text{Co}_x\text{As})_2$ in respective concentration ranges should coincide, which is consistent with the experiment (Fig. 4e [12,13]). At the same time, comparison of the phase diagrams for $\text{LaFeAsO}_{1-x}\text{F}_x$ and other $\langle 1111 \rangle$ compounds ($\text{SmFeAsO}_{1-x}\text{F}_x$ and $\text{CeFeAsO}_{1-x}\text{F}_x$) [27] demonstrates significant discrepancies in the positions of the superconducting domes. These discrepancies, as shown in Ref. [28], are due to a difference in the real content of fluorine in specimens of $\text{SmFeAsO}_{1-x}\text{F}_x$ and $\text{CeFeAsO}_{1-x}\text{F}_x$ from the nominal content determined by the initial weight. Meanwhile, in $\text{LaFeAsO}_{1-x}\text{F}_x$ the real content of fluorine coincides with the nominal value. With respective corrections made, the regions of the superconducting domes on the phase diagrams of all three compounds coincide [28].

F. $\text{Ba}_{1-x}\text{K}_x\text{Fe}_2\text{As}_2$

Consider now the hole-doped compound $\text{Ba}_{1-x}\text{K}_x\text{Fe}_2\text{As}_2$. Substitution of K for Ba leads to the emergence in one of the two FeAs planes of a hole that imparts the charge q^* to each of four nearest As ions (Fig. 9a). Localization of the doped holes on As ions is indirectly confirmed by the results of [29], where the contribution of electron carriers to thermal conductivity was observed in $\text{Ba}_{1-x}\text{K}_x\text{Fe}_2\text{As}_2$ up to $x = 0.88$). Thus, four exions are formed around each projection of K ion. The most optimal for forming HL centres, as is seen from Fig. 9b, is to order projections of the dopant into a $\sqrt{5} \times \sqrt{5}$ superlattice. The corresponding optimal concentration of the dopant is $x = 0.4$ (with account for the fact that only each second K ion dopes a hole into the given FeAs plane), which agrees well with the phase diagram of $\text{Ba}_{1-x}\text{K}_x\text{Fe}_2\text{As}_2$ (Fig. 9 [14]).

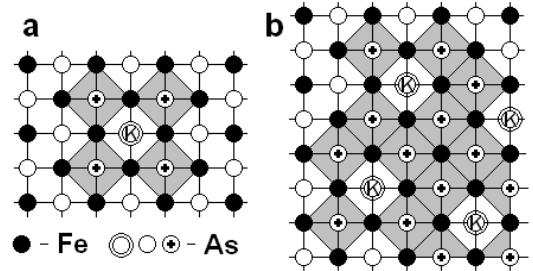


Figure 9. (a) Formation of exions in $\text{Ba}_{1-x}\text{K}_x\text{Fe}_2\text{As}_2$. Open circles indicate projections of As ions at the vertices of the tetrahedra onto the Fe plane; double circled K symbols are K ion projections on the Fe plane. Circled plus symbols are As ions carrying charge q^* . They are exion centres. (b) formation of a percolation cluster of HL centres on a $\sqrt{5} \times \sqrt{5}$ square superlattice; Exions that form HL centres are shaded

G. $\text{Ca}_{1-x}\text{La}_x\text{Fe}_2\text{As}_2$

In this compound substitution of La for Ca leads to the emergence in one of the two FeAs planes of an electron that imparts the charge q^* ($\approx -|e|/4$) to each of four nearest Fe ions (Fig. 10a). Thus, eight exions are formed around La ion projection in one of the two FeAs planes.

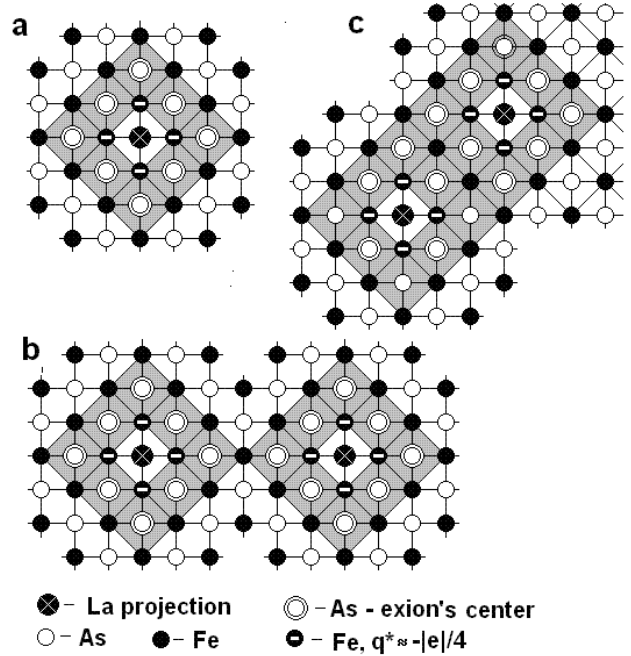


Figure 10. (a) Formation of exions (shaded) in $\text{Ca}_{1-x}\text{La}_x\text{Fe}_2\text{As}_2$. Eight exions are formed around La ion projection in one of the two FeAs planes; (b) formation of a percolation cluster of HL centres on a $\sqrt{18} \times \sqrt{18}$ superlattice; (c) formation of a percolation cluster of HL centres on a 3×3 superlattice.

At an ordered arrangement of dopants in a $\sqrt{18} \times \sqrt{18}$ superlattice we will have a percolation network of HL centres (Fig. 10b). A concentration corresponding to the percolation threshold is $x = 0.067$ (with account for the fact that only each second La ion dopes an electron into the given FeAs plane), which is in agreement with the experimental phase diagram of $\text{Ca}_{1-x}\text{La}_x\text{Fe}_2\text{As}_2$ (Fig. 4g). The most optimal for forming HL centres, as is seen from Fig. 10c, is to order projections of the dopant into a 3×3 superlattice. The corresponding optimal concentration of the dopant is $x = 0.22$ (with account for the fact that only each second La ion dopes an electron into the given FeAs plane), and the percolation threshold is $x = 0.13$ that agrees well with the phase diagram of $\text{Ca}_{1-x}\text{La}_x\text{Fe}_2\text{As}_2$ (Fig. 4g [15]).

Thus, as we have shown the regions of concentrations corresponding to the superconducting dome on the phase diagrams of cuprates and pnictides coincide with the formation regions of HL centres we introduced. The fact that this approach to the construction of phase diagrams proved to be similarly successful for cuprates and pnictides serves a serious argument in favour of the common nature of the superconducting state in these classes of HTSCs. Note also that this consideration does not rule out the possibility that compounds exist in which the proposed pairing mechanism is realized already in the undoped phase (e.g., LiFeAs), as well as in the case of isovalent substitution if the dopant locally decreases Δ_{ib} and becomes an exion centre (e.g., $\text{BaFe}_2(\text{As}_{1-x}\text{P}_x)_2$).

IV. GENERATION OF FREE CARRIERS AND MECHANISM OF SUPERCONDUCTIVITY

We now return to the consideration of the phase with $\Delta_{ct}=0$, in which an exion is formed on each cation (in cuprates) or anion (in pnictides). Let there be two exions centred at the nearest Cu cations (in cuprates) or As anions (in pnictides). They, in our assumption, form a so called HL centre, which can be considered to be a solid state analogue of the hydrogen molecule. At this centre, two electrons and two holes can form a bound state due to the possibility for two holes (electrons) in singlet state to be in the space between the central ions and be attracted simultaneously to two electrons (holes) occurring on these ions. An additional decrease of energy ΔE_{HL} can in our case be assessed from the ratio $\Delta E_{HL} \sim \Delta E_{H_2} / \epsilon_\infty^2 \approx 0.2$ eV, where $\Delta E_{H_2} = 4.75$ eV is the binding energy in the molecule of H_2 , and $\epsilon_\infty \approx 4.5-5.0$ (for cuprates) [30]. An HL centre will be considered to be occupied if both electron (hole) states on the central Cu cations (As anions) are occupied.

Thus, two electrons on Cu cations (two holes on As anions) will have lower energy if they occupy the

neighbouring cations (anions), and two holes (two electrons) linked with them are on the surrounding O anions (Fe cations). Since these pair states are essentially bosonic, they occupy a common pair level of HL centres. Herewith, as we point out above, in the phase with $\Delta_{ct}=0$ the L-states of electrons in cuprates and d-states of holes in pnictides (Fig. 2) are a superposition of the band and exciton states. Transitions of electron (hole) pairs from such a band to the HL centres and back provide for the pair hybridization of band states and the pair level of HL centres.

Consider now a possible mechanism for the generation of additional carriers in such a system. This issue is especially topical for cuprates, which in undoped state are insulators. Continuing the analogy with the hydrogen molecule, we note that, besides the H_2 molecule, there is also the bound state of two protons and one electron, namely, the H_2^+ ion. In our case, this corresponds to an ionized HL centre, on which two electrons and one hole (in cuprates) or two holes and one electron (in pnictides) form a bound state. An emerging hole (in cuprates) or an electron (in pnictides) can transit from site to site, thus providing for the overlap of the corresponding orbitals and the formation, on the level of chemical potential μ , of a hole (electron) subband of HL centres with the corresponding type of conductivity. The pair level in a one-electron scheme will correspond to (1) two states $D^{n+1}l^-$, where D are electrons on the neighbouring Cu cations, and l^- are band oxygen holes (in cuprates) or (2) L^-d^{n+1} , where L^- are holes on the neighbouring As anions, and d^{n+1} are band electrons on Fe orbitals (in pnictides).

The corresponding one-electron band structures of cuprates and pnictides are schematically shown in Fig. 11

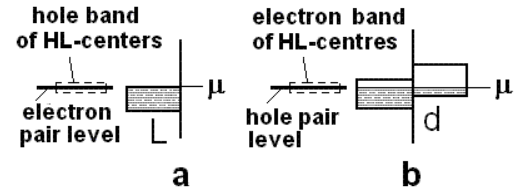


Figure 11. One-electron band structure schemes of (a) cuprates (in electron representation) and (b) pnictides (in hole representation). μ , the level of chemical potential. The electron (hole) states in the L band (d band) represent a superposition of the band and exciton states. Hole (electron) band of HL centres is formed at $T > 0$ as result of occupation of HL centres.

The concentration of carriers in the emerging band will be determined by the occupation of HL centres, i.e., by the balance between the transition rates of electron (hole) pairs to HL centres and the rates of their departure to the band as the result of the breakdown of a pair state. The value of pair hybridization Γ (or the inverse lifetime of a pair state) depends on temperature [31,32] as

$$\Gamma \approx kT \cdot (V/E_F)^2$$

(here V is the single-particle hybridization constant; E_F , Fermi energy; T , temperature). The inverse process is determined by the rate of electron–electron scattering; its rate is $\propto T^2$. Hence, for the occupation of an HL centre, η , we have:

$$\eta = 2T/(T + T_0),$$

where T_0 is a temperature-independent constant. Correspondingly, for the concentration of additional carriers $n = 2NT/(T + T_0)$, where N is the concentration of HL centres [8]. From this relation, it follows that at $T = 0$ the concentration of additional free carriers $n = 0$. (Here we assume that at $T = 0$ the occupation of HL centres is negligibly small).

As for the mechanism of superconductivity in cuprates and pnictides, we think that the superconducting pairing occurs due to the formation of a bound state of two electrons (holes) getting to the central cations (anions) of an unfilled HL centre and of two holes (electrons), with necessity emerging on adjacent ions in the phase with $\Delta_{ct} = 0$. That is, in considering the motion of electrons (holes), emerging holes (electrons) play the role of phonons in conventional superconductors.

We note once again that the occupation of HL centres with real electron (hole) pairs decreases with decreasing temperature (as the concentration of additional free carriers does). Therefore, for this mechanism to be realized the occupation of HL centres should become sufficiently small to provide for the coherence to be established within the entire volume. The superconductivity of a separate domain can be taken to require percolation over unoccupied HL centres, i.e., their occupation with real pairs should not exceed 0.4 [26].

In accordance with the model, the superconducting state breaks down at some temperature $T = T_c$, at which the number of unfilled HL centres becomes insufficient for the superconducting coherence to be established within the entire volume [33]. This property manifests itself most clearly in the underdoped cuprates, where the percolation cluster of HL centres breaks up into finite clusters, whose average size decreases with the doping decreasing [33]. Under these conditions, fluctuations in the occupation of HL centres sharply increase, which leads to the emergence of various pseudogap anomalies [33].

IV. CONCLUSION

In this work we propose a model of doping cuprates and pnictides based on the views of the self-localization of doped carriers as a consequence of their interaction with CT excitons. In the model, upon achievement of a certain dopant concentration, a percolation cluster of the phase is formed, in which the band states resonantly interact with the exciton states. This approach makes it possible to introduce into the description local atomic complexes (HL centres) occurring in the basal plane and representing pairs of like-sign neighbouring ions surrounded by ions of the other sign (the solid state analogue of the hydrogen molecule). On this centre, two electrons and two holes can form a bound state due to the possibility of two holes (in cuprates) or two electrons (in pnictides) in singlet state to be in space between the central ions and to be attracted simultaneously to two electrons (holes) occurring on these ions. The HL centres are assumed to be centres of superconducting pairing. The geometry of HL centres' arrangement in the basal plane of the crystal is determined by its crystal structure and the type of dopant, so the dopant concentration range corresponding to the existence of the percolation cluster of HL centres can be readily determined for each particular compound. We take this range for the region of a superconducting dome. To support the proposed model, we determined the specified concentration ranges for a number of well investigated HTSCs and compared the calculated domes of superconductivity with the experimental data. The good coincidence of the calculated and experimental phase diagrams may serve as a validation of the proposed model. Proceeding from this, we discussed the nature of current carriers in normal state and the features of electron pairing mechanism that can be realized in a system where band electrons resonantly interact with CT excitons. Some features of the properties of underdoped and overdoped HTSC phases that follow from the proposed model were also considered.

ACKNOWLEDGEMENTS

The authors are grateful to A.A. Gorbatsevich for useful discussions. This work is supported by RFBR (Grant 14-02-0078516)

1. C. M. Varma, S. Schmitt-Rink, E. Abrahams, Charge transfer excitations and superconductivity in ionic metals. *Sol. St. Commun*, 88, 847-851 (1993)
2. K. V. Mitsen, O. M. Ivanenko, Phase diagram of $\text{La}_{2-x}\text{M}_x\text{CuO}_4$ as the key to understanding the nature of high-

- Tc superconductors. *Usp. Fiz. Nauk* 174, 545-563 (2004) [*Phys.—Usp.* 47, 493-510 (2004)]
3. D. Haskel, V. Polinger, E.A. Stern, Where do the doped holes go in $\text{La}(2-x)\text{Sr}(x)\text{CuO}(4)$? A close look by XAFS. in *High Temperature Superconductivity, AIP Conference Proceedings* 483, 241-246 (1999)

4. P.C. Hammel, B.W. Statt, R.L. Martin, F.C. Chou, D. C. Johnston, S-W. Cheong., Localized holes in superconducting lanthanum cuprate. *Phys. Rev. B* 57, 712-715 (1998);
5. H. Wadati, I. Elfimov, G. A. Sawatzky, Where Are the Extra d Electrons in Transition-Metal-Substituted Iron Pnictides? *Phys. Rev. Lett.* 105, 157004 (2010);
6. T. Berlijn, C.-H. Lin, W. Garber, W. Ku, Do Transition Metal Substitutions Dope Carriers in Iron Based Superconductors? *Phys. Rev. Lett.* 108, 207003 (2012).
7. G. Levy, R. Sutarro, D. Chevrier, T. Regier, R. Blyth, J. Geck, S. Wurmehl, L. Harnagea, H. Wadati, T. Mizokawa, I. S. Elfimov, A. Damascelli, G. A. Sawatzky, Probing the role of Co substitution in the electronic structure of iron-pnictides. *Phys. Rev. Lett.* 109 077001 (2012).
8. K. Segawa, Y. Ando, Transport anomalies and the role of pseudogap in the 60-K phase of $\text{YBa}_2\text{Cu}_3\text{O}_{7-d}$. *Phys. Rev. Lett.* 86, 4907-4910 (2001)
9. K. Kumagai, K. Kawano, I. Watanabe, K. Nishiyama, K. Nagamine, Magnetic order and evolution of the electronic state around $x=0.12$ in $\text{La}_{2-x}\text{Ba}_x\text{CuO}_4$ and $\text{La}_{2-x}\text{Sr}_x\text{CuO}_4$. *J. Supercond.* 7, 63-67 (1994).
10. Y. Krockenberger, J. Kurian, A. Winkler, A. Tsukada, M. Naito, L. Alff. Superconductivity phase diagrams for the electron-doped cuprates $\text{R}_{2-x}\text{Ce}_x\text{CuO}_4$ ($\text{R}=\text{La, Pr, Nd, Sm, and Eu}$). *Phys. Rev. B* 77, 060505(2008)
11. N. Ni, M. E. Tillman, J.-Q. Yan, A. Kracher, S. T. Hannahs, S. L. Bud'ko, P. C. Canfield, Effects of Co substitution on thermodynamic and transport properties and anisotropic H_{c2} in $\text{Ba}(\text{Fe}_{1-x}\text{Co}_x)_2\text{As}_2$ single crystals. *Phys. Rev. B*, 78, 214515 (2008)
12. Y. Kamihara, T. Watanabe, M. Hirano, H. Hosono, Iron-Based Layered Superconductor $\text{La}[\text{O}_{1-x}\text{F}_x]\text{FeAs}$ ($x = 0.05-0.12$) with $T_c = 26$ K. *J. Am. Chem. Soc.* 130, 3296-3297 (2008)
13. T. Oka, Z. Li, S. Kawasaki, G. F. Chen, N. L. Wang, G. Zheng, Antiferromagnetic Spin Fluctuations above the Dome-Shaped and Full-Gap Superconducting States of $\text{LaFeAsO}_{1-x}\text{F}_x$ Revealed by ^{75}As -Nuclear Quadrupole Resonance. *Phys. Rev. Lett.* 108, 047001 (2012).
14. Z. Li, R. Zhou, Y. Liu, D. L. Sun, J. Yang, C. T. Lin, G. Zheng. Microscopic coexistence of antiferromagnetic order and superconductivity in $\text{Ba}_{0.77}\text{K}_{0.23}\text{Fe}_2\text{As}_2$. *Phys. Rev. B* 86, 180501 (2012).
15. Y. Sun, W. Zhou, L. J. Cui, J. C. Zhuang, Y. Ding, F. F. Yuan, J. Bai, Z. X. Shi, Coexistence of two superconducting phases in $\text{Ca}_{1-x}\text{La}_x\text{Fe}_2\text{As}_2$. *AIP Advances* 3, 102120 (2013).
16. J.L Jacobsen., High-precision percolation thresholds and Potts-model critical manifolds from graph polynomials. *J. Phys. A: Math. Theor.* 47, 135001 (2014).
17. N. Poccia, M. Chorro, A. Ricci, W. Xu, A. Marcelli, G. Campi, A. Bianconi, Percolative superconductivity in $\text{La}_2\text{CuO}_{4.06}$ by lattice granularity patterns with scanning micro X-ray absorption near edge structure. *Appl. Phys. Lett.* 104, 221903 (2014).
18. Nicola Poccia, Martijn Lankhorst, Alexander Golubov, Manifestation of percolation in high temperature superconductivity. *Physica C: Superconductivity* 503, 82-88 (2014).
19. M. Bendele, A. Barinov, B. Joseph, D. Innocenti, A. Iadecola, A. Bianconi, H. Takeya, Y. Mizuguchi, Y. Takano, T. Noji, T. Hatakeda, Y. Koike, M. Horio, A. Fujimori, D. Ootsuki, T. Mizokawa & N. L. Saini. Spectromicroscopy of electronic phase separation in $\text{K}_x\text{Fe}_{2-y}\text{Se}_2$ superconductor. *Scientific Reports* 4, 5592 (2014)
20. Takagi, R. J. Cava, M. Marezio, B. Batlogg, J. J. Krajewski, W. F. Peck Jr., P. Bordet, D. E. Cox, Disappearance of superconductivity in overdoped $\text{La}_{2-x}\text{Sr}_x\text{CuO}_4$ at a structural phase boundary. *Phys. Rev. Lett.* 68, 3777-3780 (1992)
21. K.V. Mitsen, O.M. Ivanenko, Possible nature of the pseudogap anomalies in HTSC. *Zh. Eksp. Teor. Fiz.* 134, 1153-1166 (2008) [*JETP* 107, 984-995 (2008)].
22. T. Nagano, Y. Tomioka, Y. Nakayama, K. Kishio, K. Kitazawa, Bulk superconductivity in both tetragonal and orthorhombic solid solutions of $(\text{La}_{1-x}\text{Sr}_x)_2\text{CuO}_{4-d}$. *Phys. Rev. B* 48, 9689-9696 (1993)
23. K. V. Mitsen, O. M. Ivanenko, The possible origin of incommensurate spin textures in HTSC, *Eur. Phys. J. B* 52, 227-231 (2006)
24. Y. Krockenberger, J. Kurian, A. Winkler, A. Tsukada, M. Naito, L. Alff. Superconductivity phase diagrams for the electron-doped cuprates $\text{R}_{2-x}\text{Ce}_x\text{CuO}_4$ ($\text{R}=\text{La, Pr, Nd, Sm, and Eu}$). *Phys. Rev. B* 77, 060505(2008)
25. J.C. Slater, Atomic Radii in Crystals. *J. Chem. Phys.* 41, 3199 (1964)
26. K. V. Mitsen, O. M. Ivanenko, Mechanism of carrier generation and the origin of the pseudogap and 60 K phases in YBCO. *JETP Letters*, 82, 129-133 (2005);
27. Y.J. Uemura, Energy-scale phenomenology and pairing via resonant spin-charge motion in FeAs, CuO, heavy-fermion and other exotic superconductors. *Physica B* 404 3195-3201 (2009).
28. A. Kuhler and G. Behr (2010). Unification of the Electronic Phase Diagrams of the $\text{RO}_{1-x}\text{F}_x\text{FeAs}$ Compounds by Using the Real Fluorine Content. *MRS Proceedings*, 1254, 1254-L01-04, doi:10.1557/PROC-1254-L01-04.
29. M. Matusiak, T. Wolf, Multiband thermal transport in the iron-based superconductor $\text{Ba}_{1-x}\text{K}_x\text{Fe}_2\text{As}_2$. *Phys. Rev. B* 92, 214515 (2015)
30. D.R. Harshman, A.P. Mills, Jr. Concerning the nature of high- T_c superconductivity: Survey of experimental properties and implications for interlayer coupling. *Phys. Rev. B* 45 10684-10712 (1992).
31. G.M. Eliashberg, *Pis'ma Zh. Eksp. Teor. Fiz.* 46, Prilozh.1, 94 (1987) [*Sov.Phys. JETP Lett.* 46, Suppl.1, S81 (1987)].
32. I.O. Kulik, *Fiz. Nizk. Temp.* 13, 879 (1987) [*Sov. J. Low Temp. Phys.* 13, 505 (1987)].
33. K.V. Mitsen, O.M. Ivanenko, Percolation nature of the 60 K to 90 K phase transition in $\text{YBa}_2\text{Cu}_3\text{O}_{6+d}$. *JETP*, 110, 783-787 (2010).